SAND2021-15734C

Imaging Pyrometry and Optical Depth Measurements in Explosive Fireballs using High-Speed Imaging

Alex D. Brown[1], Mateo Gomez[2], Terrence R. Meyer[3], Steven F. Son[4]
Purdue University, West Lafayette, Indiana 47907

Daniel R. Guildenbecher[5]
Sandia National Laboratories, Albuquerque, NM 87185

A significant portion of the energy released by an explosive is contained in a post-detonation fireball. Quantitative characterizations of in situ optical properties are needed to verify predictive models of these environments. This work investigates the narrowband red, green, and blue (RGB) emissive and absorptive characteristics of lab scale explosive blasts. Experiments utilize a custom triple-bandpass filter to image blast emission with a high-speed color camera and calculate temperatures from the RGB band ratios. The measured emission is contingent on the optical density, which is also explored with a triple-band (RGB) optical density measurement using the color camera. Time histories of the calculated emissive temperature and optical depth provide insight into the interpretation of pyrometric measurements in optically dense, particle laden combustion environments. This is applicable to many other reacting systems.

I. Nomenclature

EBW = Exploding bridgewire detonator
CMOS = Complementary metal-oxide-semiconductor
PETN = Pentaerythritol tetranitrate
RDX = 1,3,5-Trinitroperhydro-1,3,5-triazine
RGB = Red, green, and blue
OD = Optical density

II. Introduction

Explosives are widely-used in defense applications, industrial sectors like mining and construction, and for environmental purposes such as quenching oil fires [1]. Detonations produce gases that rapidly expand and mix with surrounding materials, resulting in a blast wave [2]. These high-temperature, high-speed flow fields often feature regions with a significant volume fraction of small particles and reactive gasses. The result is a shock-driven reactive flow that exhibits secondary combustion, turbulent instabilities, and numerous anisotropic heat and mass transfer processes. Measuring and modelling explosive blast waves is complicated by these effects, as well as the large range of relevant length and time-scales observed [3].

[1] Doctoral Student, Mechanical Engineering, brow1537@purdue.edu.
[2] Doctoral Student, Mechanical Engineering
[3] Professor, Mechanical Engineering, Aeronautics and Astronautics (by courtesy), AIAA Associate Fellow
[4] Professor, Mechanical Engineering, Aeronautics and Astronautics (by courtesy), AIAA Associate Fellow
[5] Principal Member of the Technical Staff, Engineering Sciences Center, AIAA Senior Member

Emission from explosive fireballs is often significant due to the presence of radiative soot, reactive metals, and other condensed phase particles. Spatial, temporal, and/or spectrally resolved measures of the associated emission from these sources can inform understanding of the underling physical processes. In some prior work, Steward and others observed infrared emissivity changes as a function of time in combusting and non-combusting plumes from muzzle blasts [5]. Significant effort by Gordon, Gross, and others has measured and modelled the emission of explosive blasts in infrared wavelengths [6–10]. The observed radiation was found to include grey body emission, molecular absorption features, and time dependent emissivity. Still, post-detonation environments are extraordinary complex and as demonstrated in Ref. [4] accurate prediction of the emission characteristics remains challenging. To further improve post-detonation modeling, it is necessary to measure relevant optical quantities such as wavelength resolved radiative emission and absorption. In this work, a high-speed color CMOS camera and a custom triple-wavelength bandpass filter is used to measure these quantities in the visible wavelengths and infer temperature and emissivity in small-scale blasts.

Pyrometry Background

Pyrometry is a thermometry technique that uses the ratio of thermal radiation collected at different wavelengths to estimate emissive temperature. Color cameras have been used for imaging pyrometry in literature, with temperatures reported for embers, particles, thin-filaments, soot, condensed products of explosive blasts, and many other applications [11-15]. The basic technique utilizes the color filter array inherent to a color camera chip, typically a Bayer filter [16]. This filter consists of a grid of red, green, and blue (RGB) filters that isolates the corresponding wavelength ranges onto separate pixels. After an image is collected, a demosaicing algorithm is used to assign RGB values to each pixel. To infer temperature, a gray body approach is common, in which the ratios between the RGB values are assumed to follow a gray body distribution (i.e., no wavelength dependence in emission). Under that assumption, temperature is calculated from the ratio between collected wavelength intensities as

$$T = \left[\frac{k}{hc} \frac{\lambda_1 \lambda_2}{\lambda_2 - \lambda_1} \left(\ln\left(\frac{I_2}{I_1} \frac{\eta_1}{\eta_2}\right) - 5 \ln\left(\frac{\lambda_1}{\lambda_2}\right) \right) \right]^{-1}, \quad (1)$$

where k is the Boltzmann constant, h is Planck's constant, c is the speed of light, λ_1 and λ_2 are two of the wavelengths measured, I_1 and I_2 are the corresponding measured intensities, and η_1 and η_2 are calibration constants relating the relative collection efficiency of the system. This equation is derived using Wien's approximation applied to Planck's law following the approach given in [15].

Typically, there is significant spectral overlap between RGB filters that convolves the three colors (Figure 1a): Some red light is incorrectly reported as blue or green, etc. To reduce this overlap, a combination of a custom three-wavelength bandpass filter and near-infrared blocking filters has been demonstrated to further isolate the wavelength bands that reach the camera chip (Figure 1b), following the approach developed by McNesby [16].

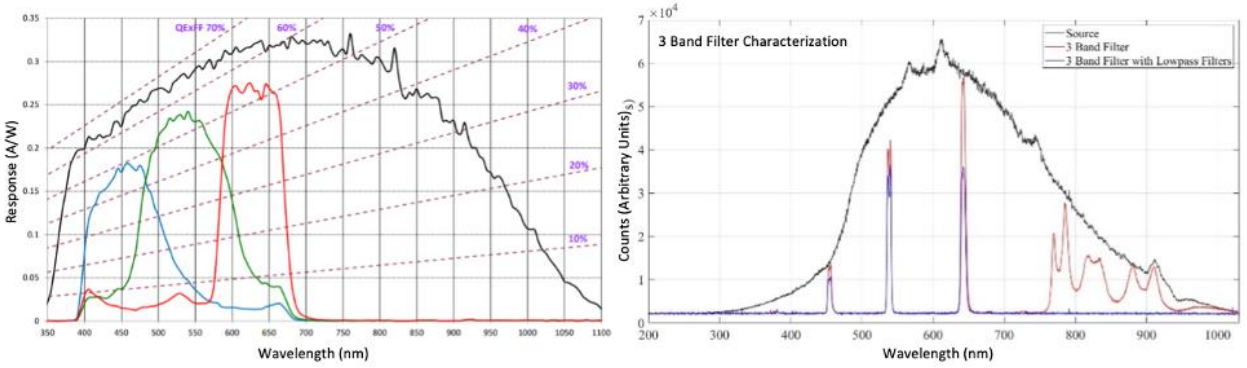

(a) (b)

Figure 1. (a) A characteristic quantum efficiency curve of a sample color camera, provided by a manufacturer. (b) Example transmission spectrum of the custom three band filter and IR blocking filters from a black body source [16].

Optical Density Background

Blasts have been demonstrated by Peuker and others to be optically dense [17]. Optical density is relevant in that it describes the amount of emissive light that may be observed from the blasts, hence how deep the collected light originates. The optical density (OD) of a medium is defined as

$$OD = \log_{10} \frac{I}{I_0}, \tag{2}$$

where I is the light intensity transmitted through the medium, and I_0 is incident light intensity. By measuring the OD of the blast at the separate RGB wavelengths, the wavelength dependence of the fireball emissivity can be studied. The optical density of small-scale blasts produced by an exploding bridgewire (EBW) detonator has previously been studied at visible wavelengths utilizing photodiodes by Lodes et al [18]. The approach in the current work is similar; however, the use of a camera chip allows for the beam to be integrated across many pixels and helps to alleviate effects of signal loss due to beam steering, although photodiodes may be capable of faster sampling rates than current cameras allow.

Various laser diagnostic techniques are available that may be useful for the study of condensed phase species, soot, or gaseous products in post-detonation blasts include planar laser induced fluorescence, laser induced incandescence, or multiple angle scattering. The wavelength dependent OD of a post-detonation blast will affect these measurements. Incident laser light will be attenuated as it travels through the blast, diminishing in intensity. The resultant fluorescence, incandescence, or scattering signal produced will also be attenuated before reaching a camera sensor. For the application of imaging pyrometry, the OD will affect the depth into the blast that a camera system will collect light. A high optical density will result in a temperature measurement on the surface of the blast, while a lower optical density will result in a temperature that is path averaged into the fireball.

III. Experimental Configuration

Experiments were performed in an optically accessible blast chamber at Purdue University. A high-speed color camera (iX Cameras, i-SPEED 5) capable of recording at speeds up to 200 kHz was used for initial pyrometry experiments and OD measurements. Pyrometry utilized the triple band filter and IR lowpass filters specified in [16].

To perform optical depth measurements, three 4.5 mW laser diodes at 450 nm, 532 nm, and 640 nm (Thorlabs) were aligned with roughly 0.3° offsets from center and made to intersect at the probe volume. To reduce signal contamination by fireball emission, the three lasers were passed through the triple bandpass and IR filter. In addition, neutral density filters were used to saturate the camera by a factor of ten, extending the dynamic range of OD measurements by a factor of 1.0 OD. 200 kHz OD measurements are performed at three locations in the fireball: one in the centerline, one offset by 12.7 mm from the centerline, and the finally one offset by 22 mm from the centerline. In select experiments, simultaneous visible emission imaging was performed using a Shimadzu HPV-X2 operating at 2 million frames per second.

Fireballs were generated by commercial RP80 EBW detonators initiated by an FS-43 capacitor discharge unit (CDU), both produced by Teledyne RISI. An RP80 consists of a gold bridgewire that vaporizes and forms a plasma during a high voltage discharge from the CDU. A reaction wave forms in an initiating 80 mg pellet of PETN that is in contact with the bridge-wire. The ensuring detonation further initiates an output pellet consisting of 123 mg of RDX. Details of EBW functionality can be found in [19].

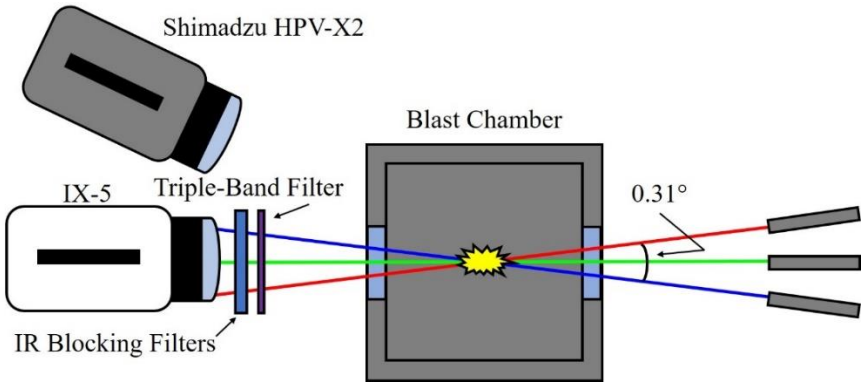

Figure 2. Experimental configuration illustrating the optical density measurement approach with a high-speed color camera and high-speed monochrome camera.

IV. Results and Discussion

Pyrometry

The calibration procedure developed by McNesby was used to correct each RGB value to obtain accurate pyrometric measurements [21]. The calibration includes two major steps. First, the spectral overlap of each of the channels was determined using the 450 nm, 532 nm, and 640 nm laser diodes used for OD measurement. This produced values for monochromatic light falsely reported as another color, i.e. 532 nm light falsely measured by the camera as either 450 nm or 640 nm. Using the algebraic methods laid out by McNesby, a corrected intensity value of each color channel was calculated that reduced the effects of spectral overlap. Second, an IR-563/201 blackbody source manufactured from Infrared Systems Development Corporation was used to calibrate the response of the camera system to a blackbody at 1000 K. Temperatures were then calculated from the 1000 K blackbody images using Equation (1), and were not found to be accurate to 1000 K. Holding the green channel signal arbitrarily constant, the red and blue channels were further corrected to bring the temperature calculation to 1000 K. The resultant calibration factors are a combination of spectral overlap corrections and the blackbody corrections.

Experimental blast images were exported as raw grayscale 12-bit files in order to avoid the use manufacturer-specific demosaicing algorithms, the details of which were unknown. The grayscale images are instead converted to RGB using a gradient-corrected linear interpolation demosaicing algorithm proposed by Malvar et al. [20]. Upon successful demosaicing, pixels are discarded if any RGB values are either saturated or have a signal level below the approximate camera noise floor (100 counts in this work). At this stage, the calibration factors were applied to correct the values for each color channel.

Using the ratios of green light to both red and blue, two independent temperatures are calculated from Equation (1). A raw grayscale image and a calculated temperature of a post-detonation blast produced by an RP80 detonator at 13 μs post-initiation are shown in Figure 3. The temperature reported is the average of the two independent temperature calculations from the green-red and green-blue ratios. Effects of the demosaicing algorithm can be seen, where interpolated values were thrown out from saturation or not meeting the signal threshold.

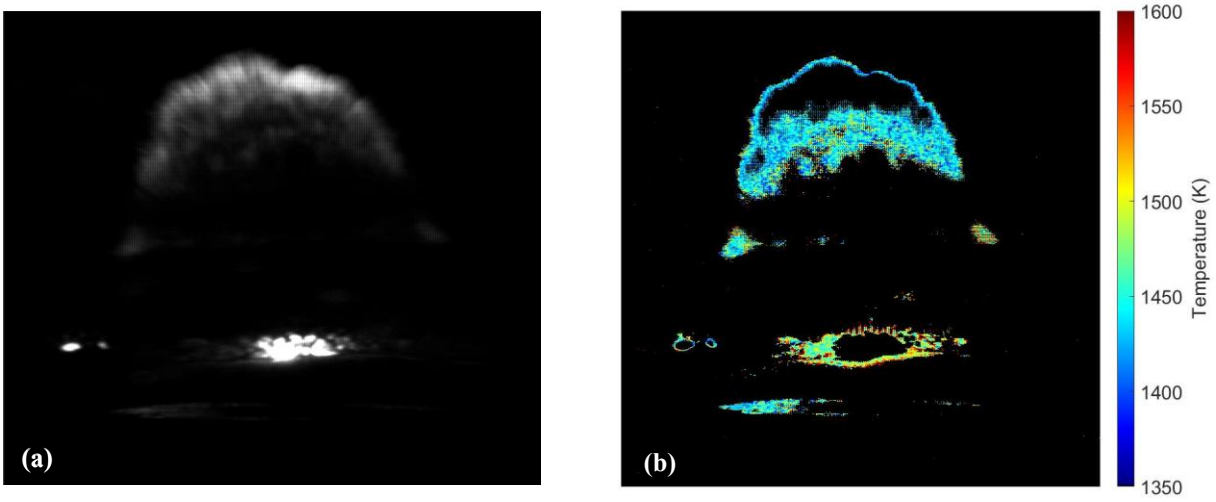

Figure 3. (a) Raw grayscale image captured on the color camera and (b) Calculated 2D temperature field.

The color camera could record at a maximum of 20 kHz. Due to the rapid evolution of the fireball, only one quality image was obtained for each blast since visible emission had largely diminished by the second frame. To construct a time-resolved mapping of pyrometric temperatures, the camera was delayed in 5 µs increments, starting at 13 µs. Three images are shown in Figure 4 that highlight the evolution in post-detonation blast morphology.

As the blast progresses, calculated pyrometric temperatures slightly increase, which is also reflected in Coherent anti-Stokes Raman scattering (CARS) gas-phase temperature measurements performed by Richardson in an identical environment, although average calculated temperatures are slightly higher in this work [21]. The observed temperature increase may suggest that exothermic reactions continue to play an important role in the energy release of the blast, even at later times. For comparison with the gas phase measurements, Figure 5 provides histograms of condensed phase pyrometric temperatures at identical times to those studied by Richardson. The disagreement in the condensed phase dominated temperatures with gas phase temperatures is a topic worthy of further exploration to determine if the discrepancy is due to the accuracy of the two measurement techniques or a real physical difference in phase kinetics.

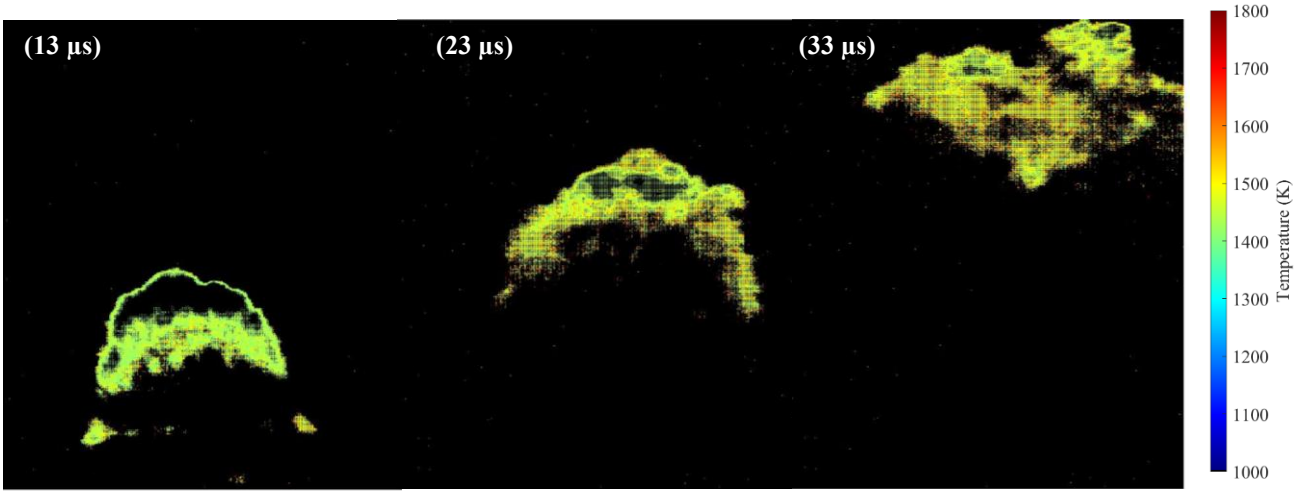

Figure 4. A sample time history of pyrometric temperatures.

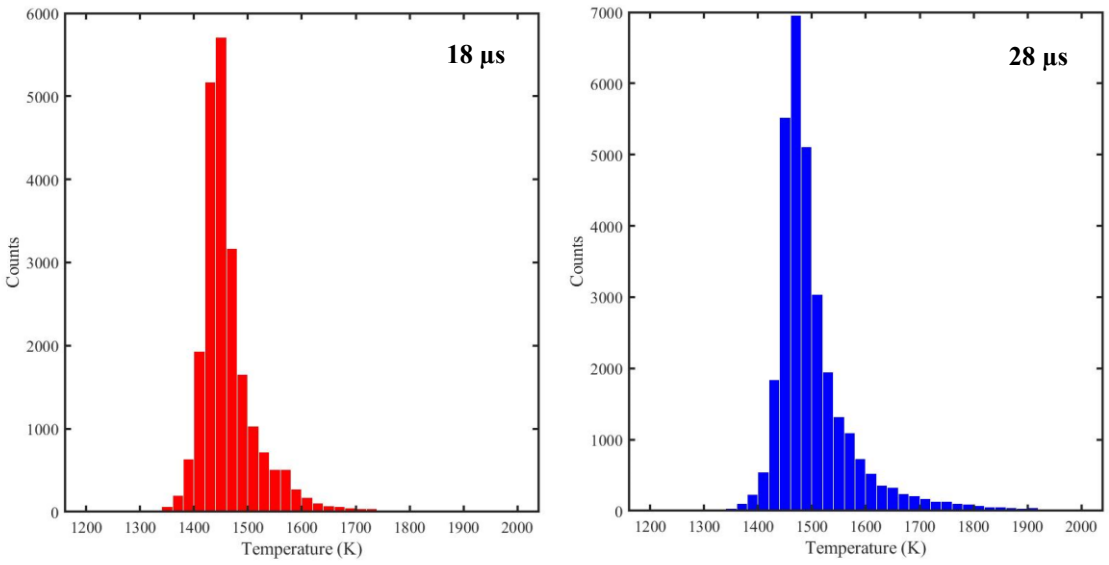

Figure 5. Pyrometric temperature histograms at two different times after detonator initiation.

Optical Density

To calculate optical density, the incident laser light intensity was measured on the camera chip. This was done by slightly undersaturating the camera below the 12-bit depth of the camera with an OD 1.0 filter in front of the camera. When the OD 1.0 filter was removed, the camera signal was saturated by a factor of 10. The baseline values for I_0 are calculated by multiplying the counts in the undersaturated images by 10. Values of I for each frame are quantified by summing the individual RGB color channels during in-situ tests. The beams are slightly offset on the camera chip as they diverge at the 0.3° incident angle and were easily distinguished during processing. Furthermore, each pixel was examined to determine which RGB channel was dominant, such that each pixel was assigned as a red, green, or blue pixel. In this way, the effects of beam steering are minimized. During the experiment, changes in index of refraction and any vibrations due to the blast caused the beams to wander slightly on the camera chip but did not reach the boundary of the chip. As a result, the entirety of each laser beam is imaged without loss of signal, which may not be as easily accomplished with single element sensors such as photodiodes.

Calculated OD at each wavelength during a single blast are shown in Figure 6. OD traces at 640 nm at three horizontal locations in the post-detonation blast are shown in Figure 7. At early fireball times, centerline optical densities exceed 3, meaning that less than one thousandth of incident light is able to penetrate the fireball. This is followed by a sharp drop in OD and a subsequent rise at later times. At the two offsets, optical densities do not match what is seen in the centerline, suggesting a sharp drop off in OD with radial location, which is expected. Optical densities are similar for the three wavelengths used at later times as the post-detonation products circulate in the blast chamber, although at early times during the blast, there appears to be resolvable differences. At early times with high optical densities, visible imaging and pyrometry is dominated by the outer shell of the blast, as light in the interior of the fireball will be significantly absorbed. At later times, when optical density has deteriorated, the camera sensor integrate signal further into the fireball.

The presented measurements are point measurements, but by expanding the laser beams to full fill the camera chip, it may be possible to image spatially resolved optical densities at the RGB wavelengths in future work.

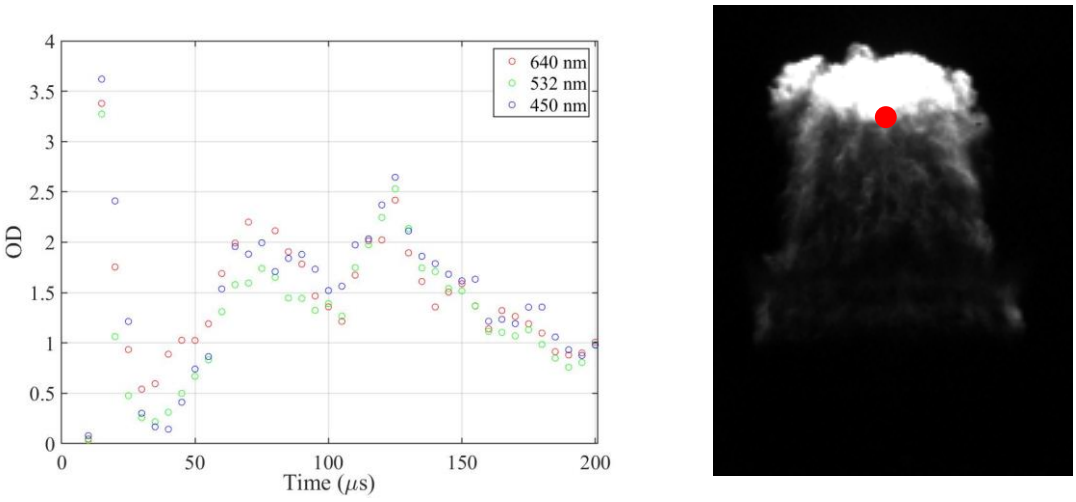

Figure 6. (a) Selected centerline optical density time history and (b) Location of laser beams (red circle) located on the blast at 15 µs.

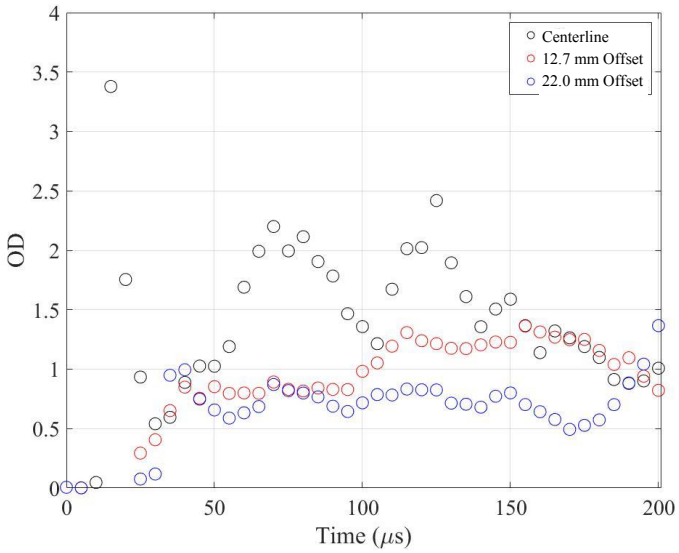

Figure 7. 640 nm OD at three different post-detonation fireball locations.

V. Conclusion

Pyrometric temperatures and optical densities in benchtop-scale post-detonation blasts were experimentally measured using a high-speed color camera, taking advantage of the built-in color filter. Pyrometry reveals a slight increase in condensed phase temperatures on the outer shell of the blast as the blast evolves, which is also evident in post-detonation gas phase temperatures measured in literature. More work is needed to fully understand the relationship between gas phase and condensed phase temperatures, in which there is some disagreement. Optical densities are high at early times in the centerline of the blast, where less that a thousandth of laser light penetrates the blast. High optical densities were resolved by intentionally saturating the color camera by a known factor. On the edges of the blast, absorbance is lower. As a result, pyrometric measurements in the centerline are biased towards the outer layer of the blast but will integrate more of the blast on the edges. More work is needed to fully understand optical density at other wavelengths, which could be achieved using additional custom filters.

The use of a color camera and custom optical filters is shown to be an applicable tool for the quantification of both emissive and absorptive quantities of post-detonation blasts. As camera technology evolves, color cameras capable of higher framing rates will allow for the time-resolved measurement of these quantities using the demonstrated techniques.

Acknowledgements

This paper describes objective technical results and analysis. Any subjective views or opinions that might be expressed in the paper do not necessarily represent the views of the U.S. Department of Energy or the United States Government. The support of the Laboratory Directed Research and Development program at Sandia National Laboratories is gratefully acknowledged. Sandia National Laboratories is a multimission laboratory managed and operated by National Technology & Engineering Solutions of Sandia, LLC, a wholly owned subsidiary of Honeywell International Inc., for the U.S. Department of Energy's National Nuclear Security Administration under contract DE-NA0003525.

The authors would like to thank Dr. Kevin McNesby of the US Army Research Laboratory for collaboration and procurement of the triple-band wavelength filter.

References

[1] S. Meyers and E. S. Shanley, "Industrial explosives - a brief history of their development and use," *Journal of Hazardous Materials*, vol. 23, no. 2, pp. 183-201, 1990.

[2] C. M. Jenkins, "Explosively driven particle fields imaged using a high speed framing camera and particle image velocimetry," *Int. J. Multiph. Flow*, p. 14, 2013.

[3] M. J. Kaneshige, M. R. Baer, and M. A. Cooper, "Understanding multi-phase and multi-scale aspects of unconventional blast events," Sandia Report SAND2006-6515C, 2006.

[4] B. J. Steward, G. P. Perram, and K. C. Gross, "Modeling midwave infrared muzzle flash spectra from unsuppressed and flash-suppressed large caliber munitions," *Infrared Phys. Technol.*, vol. 55, no. 4, pp. 246–255, Jul. 2012, doi: 10.1016/j.infrared.2012.04.005.

[5] D. R. Guildenbecher, A. R. Dallman, E. M. Hall, B. R. Halls, Elizabeth M. C. Jones, S. P. Kearney, R. T. Marinis, C. Murzyn, D. R. Richardson, F. Perez, P. L. Reu, A. D. Thompson, M. C. Welliver, "Advancing the science of explosive fragmentation and afterburn fireballs though experiments and simulations at the benchtop scale," Sandia Report SAND2020-9893, 1669203, 690957, Sep. 2020. doi: 10.2172/1669203.

[6] J. M. Gordon, K. C. Gross, and G. P. Perram, "Temperature dynamics of aluminized cyclotrimethylenetrinitramine fireballs for event classification," *Opt. Eng.*, vol. 53, no. 2, p. 021106, Oct. 2013, doi: 10.1117/1.OE.53.2.021106.

[7] J. M. Gordon, M. T. Spidell, J. Pitz, K. C. Gross, and G. P. Perram, "High speed spectral measurements of IED detonation fireballs," Orlando, Florida, Apr. 2010, p. 76650S. doi: 10.1117/12.850177.

[8] J. M. Gordon, K. C. Gross, and G. P. Perram, "Temporally resolved infrared spectra from the detonation of advanced munitions," Orlando, Florida, USA, May 2009, p. 733006. doi: 10.1117/12.818166.

[9] K. C. Gross, J. Wayman, and G. P. Perram, "Phenomenological fireball model for remote identification of high-explosives," Orlando, Florida, USA, Apr. 2007, p. 656613. doi: 10.1117/12.719977.

[10] K. C. Gross, G. P. Perram, and R. F. Tuttle, "Modeling infrared spectral intensity data from bomb detonations," Orlando, Florida, USA, May 2005, p. 100. doi: 10.1117/12.603206.

[11] D. K. Kim and P. B. Sunderland, "Fire ember pyrometry using a color camera," *Fire Saf. J.*, vol. 106, pp. 88–93, Jun. 2019, doi: 10.1016/j.firesaf.2019.04.006.

[12] H. Lu *et al.*, "Particle surface temperature measurements with multicolor band pyrometry," *AIChE J.*, vol. 55, no. 1, pp. 243–255, Jan. 2009, doi: 10.1002/aic.11677.

[13] P. B. Kuhn, B. Ma, B. C. Connelly, M. D. Smooke, and M. B. Long, "Soot and thin-filament pyrometry using a color digital camera," *Proc. Combust. Inst.*, vol. 33, no. 1, pp. 743–750, 2011, doi: 10.1016/j.proci.2010.05.006.

[14] J. M. Densmore, M. M. Biss, K. L. McNesby, and B. E. Homan, "High-speed digital color imaging pyrometry," *Appl. Opt.*, vol. 50, no. 17, p. 2659, Jun. 2011, doi: 10.1364/AO.50.002659.

[15] Y. Chen *et al.*, "Study of aluminum particle combustion in solid propellant plumes using digital in-line holography and imaging pyrometry," *Combust. Flame*, vol. 182, pp. 225–237, Aug. 2017, doi: 10.1016/j.combustflame.2017.04.016.
[16] McNesby K, Dean S, Benjamin R, Grant J, Anderson J, Densmore J. Imaging pyrometry for most color cameras using a triple pass filter. Rev Sci Instrum. 2021 Jun 1;92(6):063102. doi: 10.1063/5.0037230. PMID: 34243502.
[17] J. M. Peuker, P. Lynch, H. Krier, and N. Glumac, "Optical depth measurements of fireballs from aluminized high explosives," *Opt. Lasers Eng.*, vol. 47, no. 9, pp. 1009–1015, Sep. 2009, doi: 10.1016/j.optlaseng.2009.04.011.
[18] R. Lodes, H. Krier, and N. Glumac, "Spectrally- and Temporally-Resolved Optical Depth Measurements in High Explosive Post-Detonation Fireballs," *Propellants Explos. Pyrotech.*, vol. 45, no. 3, pp. 406–415, Mar. 2020, doi: 10.1002/prep.201900225.
[19] P. J. Rae and P. M. Dickson, "A review of the mechanism by which exploding bridge-wire detonators function," *Proc. R. Soc. Math. Phys. Eng. Sci.*, vol. 475, no. 2227, p. 20190120, Jul. 2019, doi: 10.1098/rspa.2019.0120.
[20] H. S. Malvar, Li-wei He, and R. Cutler, "High-quality linear interpolation for demosaicing of Bayer-patterned color images," in *2004 IEEE International Conference on Acoustics, Speech, and Signal Processing*, Montreal, Que., Canada, 2004, vol. 3, pp. iii-485–8. doi: 10.1109/ICASSP.2004.1326587.
[21] D. R. Richardson, S. P. Kearney, and D. R. Guildenbecher, "Post-detonation fireball thermometry via femtosecond-picosecond coherent anti-Stokes Raman Scattering (CARS)," *Proc. Combust. Inst.*, vol. 38, no. 1, pp. 1657–1664, 2021, doi: 10.1016/j.proci.2020.06.257.